





RESEARCH ARTICLE OPEN ACCESS

# Evaluation and Clinical Validation of Pan-Specific and Clade-Specific Diagnostic Real-Time PCR Assays for Monkeypox Virus

Hong Chang<sup>1,2</sup> | Tin Hang Hung<sup>3</sup>  | Binbin Li<sup>1</sup> | Bobby Lim-Ho Kong<sup>2</sup>  | Ashwathi Asha Madhavan<sup>2</sup> | Yue Wang<sup>1</sup> | Ming-shan Tsai<sup>2</sup>  | Dan Deng<sup>4</sup>  | Zhanfeng Cui<sup>1,5</sup>

<sup>1</sup>Oxford Suzhou Centre for Advanced Research (OSCAR), University of Oxford, Suzhou, Jiangsu, China | <sup>2</sup>ZYTCA Limited, Centre for Innovation and Enterprise, Begbroke, Oxfordshire, UK | <sup>3</sup>Department of Biology, University of Oxford, Oxford, Oxfordshire, UK | <sup>4</sup>Department of Dermatology, Shanghai Children's Medical Center, School of Medicine, Shanghai Jiao Tong University, Shanghai, China | <sup>5</sup>Institute of Biomedical Engineering, Department of Engineering Science, University of Oxford, Oxford, Oxfordshire, UK

**Correspondence:** Tin Hang Hung ([tin-hang.hung@biology.ox.ac.uk](mailto:tin-hang.hung@biology.ox.ac.uk)) and Zhanfeng Cui ([zhanfeng.cui@eng.ox.ac.uk](mailto:zhanfeng.cui@eng.ox.ac.uk))

**Received:** 18 July 2025 | **Revised:** 24 February 2026 | **Accepted:** 18 March 2026

**Funding:** National Natural Science Foundation of China, Grant/Award Number: 82173396; OSCAR ITC for Advanced Molecular Diagnostics, Grant/Award Number: YZCXPT2022204

## ABSTRACT

Human mpox, formerly known as monkeypox, has twice been declared a Public Health Emergency of International Concern (PHEIC) by the World Health Organization, in 2022 and 2024. Despite this, global access to rapid, reliable diagnostics remains limited, hindering outbreak control and equitable clinical response. To address this gap, we developed and validated a rapid direct real-time PCR assay capable of detecting and differentiating Clade I and Clade II monkeypox virus (MPXV) directly from clinical samples. We designed a new pan-specific B15L assay to complement the published F3L assay and introduced the first clade-specific assay targeting the B1R gene of Clade I MPXV. In silico validation showed that both B15L and F3L assays detected all available MPXV genomes with 100% sensitivity, while B1R selectively detected only Clade I genomes with 100% specificity. Cross-reactivity screening against 40 high-priority non-target organisms revealed minimal risk of false positives. We confirmed analytical sensitivity of 2 copies per reaction for all assays in vitro, with clade-specific B1R showing 100% specificity. When adapted into a lyophilized direct PCR format for near-point-of-care use, the assay demonstrated detection down to 1 copy per reaction for pan-specific targets and 2 copies for clade-specific detection in spiked clinical samples. This direct PCR assay delivers accurate results in under 1 h without requiring nucleic acid extraction. Our combined genomic, laboratory, and clinical validations demonstrate exceptional sensitivity and specificity, positioning this assay as a highly promising tool in emergency mpox diagnostics and a potential model for future outbreak-responsive testing platforms.

## 1 | Introduction

Human mpox, formerly known as monkeypox, has emerged as a significant public health concern, particularly highlighted by the World Health Organization's (WHO) two-time declaration of a Public Health Emergency of International Concern

(PHEIC) in May 2022 and August 2024. Infected individuals may experience fever, lymphadenopathy, and a characteristic rash that might lead to secondary infection. Immunocompromised individuals are more vulnerable to severe manifestations of the disease, and in the most severe cases, death. This zoonotic viral disease, caused by the monkeypox virus

Hong Chang and Tin Hang Hung contributed equally to this study.

This is an open access article under the terms of the [Creative Commons Attribution](https://creativecommons.org/licenses/by/4.0/) License, which permits use, distribution and reproduction in any medium, provided the original work is properly cited.

© 2026 ZYTCA Limited and The Author(s). *Journal of Medical Virology* published by Wiley Periodicals LLC.

(*Orthopoxvirus monkeypox*, also known as MPV, MPXV, and hMPXV) first isolated in laboratory monkeys in Denmark in 1958 [1], has recently seen a dramatic increase in global cases, with over 100,000 infections and 230 deaths (accessed 10 November 2024 from [https://worldhealthorg.shinyapps.io/mpx\\_global/](https://worldhealthorg.shinyapps.io/mpx_global/) [2]).

MPXV has a complex phylogenetic history, primarily categorized into two main clades: Clade I and Clade II. Clade I (formerly Congo Basin or Central African clade), with subclades Ia and Ib, is associated with higher mortality rates, while Clade II (formerly West African clade), with subclades IIa and IIb, has been linked to milder disease outcomes [3–5]. Historically, both only led to endemic outbreaks, but the recent global outbreak of mpox since 2022 was caused by an emerging lineage B.1 in the Clade IIb in Europe around May 2022 [6, 7], the first PHEIC. This lineage has shown significant genetic divergence and rapid mutation rates, raising concerns regarding its transmissibility and potential for further adaptation [8, 9]. Additionally, the emergence of Clade Ib, which causes a more widespread endemic outbreak in the Democratic Republic of Congo, has shown increased human-to-human transmission [10] and thus the second PHEIC. In November 2024, the United Kingdom confirmed the first local transmission of Clade Ib mpox outside Africa since the onset of the second PHEIC [11].

The emergence of new strains is particularly alarming as they may exhibit enhanced transmissibility and virulence, posing a substantial public health threat [12]. WHO has already added MPXV to the list of priority pathogens that might cause a pandemic. The global spread of Clade IIb, coupled with the escape of Clade I from endemic areas, underscores the necessity for vigilant surveillance to mitigate and contain the risk of a pandemic.

Molecular diagnostics plays a crucial role in mitigating the risk of a pandemic by enabling mass screening and rapid identification, as we learned from the immediate past lesson from the COVID-19 pandemic [13]. Early evidence, such as from Switzerland, demonstrated that rapid turnaround of molecular diagnostics in combination with effective contact tracing was essential in outbreak control [14]. Among various diagnostic methods available, real-time polymerase chain reaction (RT-PCR) assays remain the gold standard for their high sensitivity and specificity, especially useful for low target level when pathogen loads may still be minimal in early stages of infection [15]. The quantitative nature also offers significance in monitoring viral load and estimating infectivity [16]. However, traditional real-time PCR systems require expensive equipment and highly trained professionals to operate, significantly limiting their use to well-equipped laboratories.

The Target Product Profiles (TPP) published by WHO [17] in 2023 have highlighted the pressing need for more affordable, simplified, and decentralized diagnostic kits for mpox in outbreak regions. While several commercial mpox real-time PCR kits have been available since the PHEIC declaration in 2022, all currently require DNA extraction and purification steps to eliminate PCR inhibitors commonly found in clinical samples, only suitable for clinical laboratories when handling large volumes of tests [18]. Moreover, none of the kits approved under the WHO Emergency Use Listing (EUL) or CDC Emergency Use Authorization (EUA) can differentiate between MPXV Clades I and II, despite this being one of the preferred characteristics outlined in the WHO mpox TPPs.

The overarching goal of this paper is to develop clade-specific diagnostic primers and probes for integration into real-time PCR assay. First, we describe how we optimize the primer design algorithm based on the openly available genomic data. Second, we evaluate their sensitivity and specificity in differentiating the MPXV clades in both in silico and in vitro tests. Third, we validate the performance of our assay on human clinical samples that were spiked with synthetic MPXV DNA fragments and evaluate its analytical sensitivity.

## 2 | Methods

### 2.1 | MPXV Pan-Specific Primer Design and Screening

We downloaded all complete genomic data of MPXV (NCBI Taxon: 10244) using NCBI Datasets. We also followed the WHO instructions and requirements for emergency use listing submission on in vitro diagnostic testing of MPXV nucleic acid (PQDx\_457 version; 10 September 2024) in obtaining a list of 40 non-target high priority organisms (Supplementary Table 1), including same-family viruses such as smallpox virus, camelpox virus, and buffalopox, and other common contaminants such as herpes simplex virus, streptococcus, and human genomic DNA.

We mapped all MPXV genomic sequences to the reference genome NC\_003310.1 and conducted multiple sequence alignment using ViralMSA 1.1.30. We then designed mpox-specific primer using the real-time PCR mode in varVAMP 1.2.1 mode and screened primers that might bind to non-target genomes using blastn 2.16.0. All candidates for primers and probes were aligned to the reference and non-target genomes to inspect their sequence similarity and predict their binding efficiency. We picked the highest-confidence primers and probes targeting the **B15L** loci and obtained the primers and probes synthesized by Integrated DNA Technologies (United Kingdom). We also included another previously designed primer scheme on **F3L** [19]. Sequences and statistics for all primers and probes listed in this study could be found in Supplementary Table 2.

### 2.2 | MPXV Clade-Specific Primer Design

With reference to the previous phylogenetic study [20], 56 MPXV genomes were chosen for the clade-specific primer design. Among the 56 genomes, 2 of them were reference genomes for Clade I (NC\_003310) and Clade II (NC\_063383) MPXV, while the other 54 were public genomic resources in NCBI (Supplementary Table 3 of their accession & origin & clades in supp). We aligned the genomes by using MAFFT version 7 (<https://mafft.cbrc.jp>). Clade-specific regions were screened based on an indel observed in the B1R loci based on the multiple sequence alignment, where a ~2.5 Kb-insertion in Clade II would prevent real-time PCR amplification. We manually designed clade-specific primers and probes that flanked the **B1R** loci.

### 2.3 | Homology Analysis of Specificity

We analyzed the sequences of primers and probes of B15L, F3L, and B1R for homology with full-length genomic sequences

attained from Nextstrain. Nextstrain contained 473 Clade Ia sequences, 128 Clade Ib sequences, 25 Clade IIa sequences, and 221 Clade IIb sequences. We ran blastn 2.16.0 with the following command due to the nature of primer and probe sequences: ‘task blastn-short -word\_size 7 -evaluate 100 -perc\_identity 80 -reward 2 -penalty -3 -gapopen 2 -gapextend 1 -dust no’, which increased sensitivity for short sequences, retained alignments with weaker statistical significance, and permitted small indels with minimal penalties. We also manually crosschecked the homology results and the sequences and removed those that contained a significant number of unknown bases, as stretches of “N,” in our target amplicons. The final analyses contained 393 Clade Ia sequences, 55 Clade Ib sequences, 25 Clade IIa sequences, and 217 Clade IIb sequences.

## 2.4 | In silico Inclusivity Test for MPXV Pan-Specific Primers

We used R version 4.4.0 to analyze the homology results and potential amplification successes. First, all the homology hits from blastn were sorted based on the genomic coordinates for each of the two primer sets (B15L and F3L). Then, potential amplification success was determined if the hits from the forward primer, probe, and reverse primer, or the reverse way, were consecutive.

We then visualized two statistics. First, we calculated the sensitivity, which was calculated as the number of potential amplification successes divided by the total number of genomes tested, for each of the four sub-clades. Second, for those with potential amplification success, we calculated the sequence identity for each genomic sequence on the four sub-clades.

## 2.5 | In Silico Specificity Test for MPXV Clade-Specific Primers

We ran the same blastn command as above using B1R Clade I-specific primers and probe with the same full set of MPXV genomic sequences and the same R analysis as above to analyze potential amplification successes.

We determined potential amplification successes by both the consecutive homologies of forward primer, probe, and reverse primer, and the potential amplicon length. While there is no absolute consensus on the limit of amplicon length by real-time PCR, most guidelines recommend < 200 bp for optimal efficiency. We used < 1000 bp as the criterion for potential success.

## 2.6 | In Silico Cross-Reactivity Test With Other Non-Target Organisms

We analyzed the sequences of primers and probes for homology with full-length genomic sequences for 40 non-target high-priority organisms as above. We searched the metadata of complete genomes for each of the organisms using their NCBI Taxonomy IDs with NCBI Datasets command-line tools version 16.29.0. We then randomly selected five representative genomes for each organism and merged all the genomes into a single sequence file. List of randomly selected representative genomes

could be found in Supplementary Table 4. We ran blastn 2.16.0 with the same parameters as above.

We then used R version 4.4.0 to analyze the homology results and potential amplification successes as above.

We then visualized two statistics. First, we calculated the frequency of potential homology, which was calculated as the number of homology hits from blastn divided by the total number of genomes tested, for each of the four sub-clades. Second, we reported the average sequence similarity.

## 2.7 | In Vitro MPXV Direct Real-Time PCR Assay

For MPXV quantification in subsequent in vitro analyses, real-time PCR assays were performed with 20- $\mu$ L reactions, which contained 10  $\mu$ L 2 $\times$  Lyo PCR Master Mix (Apto-Gen Ltd, United Kingdom), 5  $\mu$ L primer-probe pre-mix (200 nM B15L and F3L pan-specific primers and 100 nM probe; or 400 nM B1R Clade I-specific primer and 200 nM probe), and 5  $\mu$ L samples (viral samples or synthetic DNA standards), using a QuantStudio 5 Real-Time PCR System (Thermo Fisher Scientific). The thermocycling profile for RT-PCR was as follows: an initial denaturation at 95°C for 1 min, followed by 40 cycles of 95°C for 10 s and 60°C for 15 s. Signal was collected after each cycle.

## 2.8 | Synthesis of MPXV Genomic Standards and Establishment of Standard Curve

We designed two synthetic standards (Integrated DNA Technologies, United Kingdom) for MPXV genomes using the multiple sequence alignment obtained from above: an 877-bp Clade I-like sequence that contained sequences of F3L, B15L, and B1R genes; and a 618-bp Clade II-like sequence that contained sequences of F3L, B15L, and D13L genes. The sequences of the MPXV synthetic standards can be found in Supplementary Table 5.

Synthetic MPXV genomic DNA standards were first diluted by 1X IDTE buffer (Integrated DNA Technologies, United Kingdom) to 10 ng/ $\mu$ L. Accurate concentration of the stock DNA standard was then determined by Qubit dsDNA Quantification Broad Range Assay Kit (Thermo Fisher Scientific). DNA copy number and dilution volume were calculated with Thermo Scientific Web Tools. Then, DNA standards were serially diluted (10-fold, from 10<sup>6</sup> to 10<sup>0</sup> copies/ $\mu$ L) and real-time PCR was performed on QuantStudio™ 5 Real-Time PCR System (Thermo Fisher Scientific, USA). Experiment was triplicated for each concentration, and the mean and standard deviation of the  $C_t$  value were calculated. In order to establish the standard curve, the mean of  $C_t$  was plotted against the log<sub>10</sub> (DNA copy number), with error bars showing the standard deviation. By using the model of linear regression, the equation, hence the slope ( $m$ ) and goodness of fit ( $R^2$ ) of the standard curve were obtained. The amplification efficiency ( $E$ ) was calculated by using the following formula:  $E = [10^{(-1/m)} - 1] \times 100\%$ .

## 2.9 | In Vitro Sensitivity for MPXV Primers

We first evaluated the analytical sensitivity of each primer set (pan-specific B15L and F3L and Clade I-specific B1R) by

determining the tentative limit of detection (LoD), which was defined as the lowest amount of target compound in a sample that could be accurately measured by the primer. We adopted the CLSI EP17-A2 guideline, which sets the standard for evaluation and documentation of the detection capability of clinical laboratory measurement procedures [21]. Real-time PCR reaction was run for each set of primer pairs. Experiment was triplicated with a range of synthetic DNA concentrations ( $2 \times 10^4$ ,  $2 \times 10^3$ ,  $2 \times 10^2$ ,  $2 \times 10^1$ ,  $2 \times 10^0$ , and  $2 \times 10^{-1}$  copies/reaction). Tentative LoD was estimated when positive detection was below 100%. To confirm the experimental sensitivity of each primer, the experiment was repeated for 20 replicates, with the sample concentration at the tentative LoD. The analytical LoD was confirmed when MPXV was positively detected in 95% of the replicates.

## 2.10 | In Vitro Specificity of MPXV Pan-Specific and Clade I-Specific Primer

In order to determine the experimental specificity of MPXV pan-specific and Clade I-specific primers, real-time PCR assays were performed with 2000-copies MPXV Clade II synthetic standard. Specificity of MPXV pan-specific and Clade I-specific primer (B1R) was then estimated by the numbers of true positives and false negatives.

## 2.11 | Acquisition and Preparation of Clinical Matrix

We obtained 50 human skin lesion swab samples from the Department of Dermatology, Shanghai Children's Medical Center, School of Medicine, Shanghai Jiao Tong University. Details of the sample types could be found in Supplementary Table 6. This study was approved by the Institutional Review Board of Shanghai Children's Medical Center (SCMCIRB-K2025018-1). Anonymised clinical samples were provided to the Oxford Suzhou Centre for Advanced Research for processing.

To prepare the MPXV-negative clinical matrix, 500  $\mu$ L of RNase-free water was added to each of the 50 swab tubes, which were then vortexed for 10 min. Then, 200  $\mu$ L of supernatant from each tube was pooled into a single 50-mL centrifuge tube, and the total volume was adjusted to 10 mL. Finally, the matrix was aliquoted and stored at  $-80^\circ\text{C}$ .

## 2.12 | Clinical Validation of Analytical Sensitivity With Spiked Standards and Irradiated Virus

We incorporated our assay into the UlfaQ™ Direct PCR system (ZYTCA Ltd, United Kingdom) (Figure 1), which contained an enhanced reaction buffer that eliminated the effects of inhibitors. We added 16  $\mu$ L of MPXV-negative clinical matrix and 25  $\mu$ L UlfaQ Sample Processing Control (SPC) into 500  $\mu$ L of UlfaQ lysis buffer, then spiked in 4  $\mu$ L of our MPXV synthetic standard. We included standards of six different concentrations (150, 125, 100, 75, 50, and 0 copy/mL) and a negative control (without SPC). We tested Clade I and Clade II separately; thus, in total, we had 14 matrices.

For each matrix, we transferred 20  $\mu$ L of the lysate into a pre-lyophilized reaction master mix (Tube A), which contained UlfaQ™ Direct PCR mix and our MPXV primers and probes. Another 20  $\mu$ L of the lysate was also added to the lyophilized internal control assay (Tube B) targeting SPC and human beta-actin gene. We performed RT-PCR on three replicates for each matrix on QuantStudio™ 5 Real-Time PCR System (Thermo Fisher Scientific). The thermocycling profile for real-time PCR was as follows: an initial denaturation at  $95^\circ\text{C}$  for 1 min, followed by 40 cycles of  $95^\circ\text{C}$  for 5 s and  $60^\circ\text{C}$  for 10 s.

The analytical sensitivity of our assay was determined in a similar approach of CLSI EP17-A2 guideline [21] as described above. Tentative LoD was estimated when positive detection was below 100%. To confirm the analytical sensitivity of each primer, the experiment was repeated for 20 replicates, with the sample concentration at the tentative LoD. The analytical sensitivity was confirmed when MPXV was positively detected in 95% of the replicates.

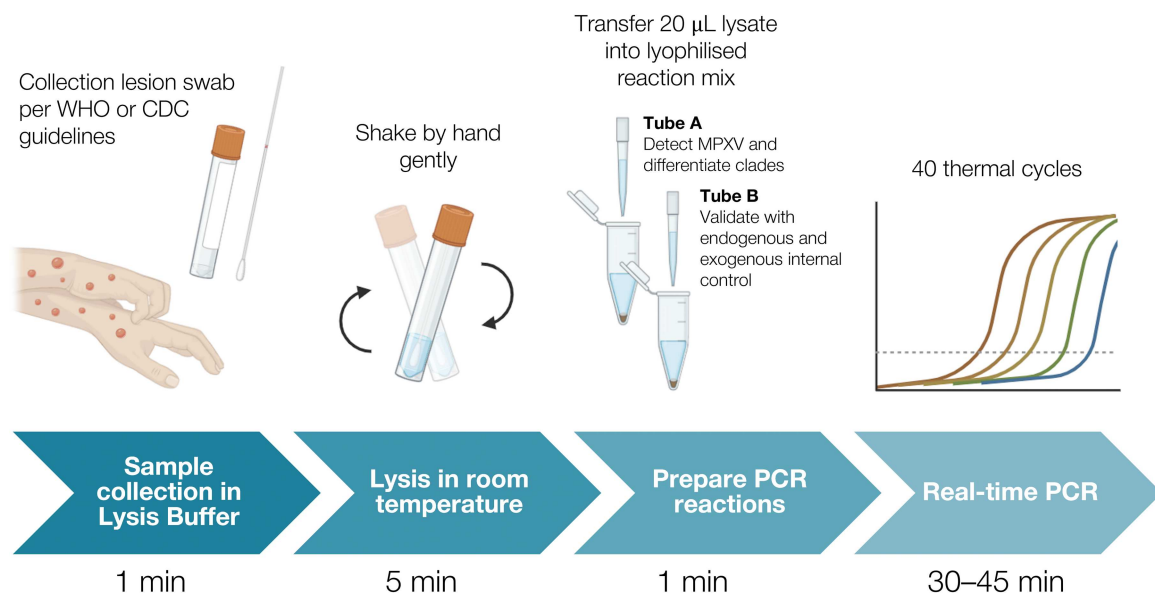


**FIGURE 1** | Graphical abstract of direct real-time PCR in clinical validation.

As a complementary analysis,  $LoD_{95}$  was estimated using probit regression. Binary detection outcomes were modeled against the input number of copies per reaction using a generalized linear model with a probit link.  $LoD_{95}$  was defined as the concentration corresponding to a predicted 95% detection probability.

In an additional experiment, we replaced the MPXV synthetic standard spike-ins with irradiated MPXV Clade II virus (2301231v) obtained from the Culture Collections of the UK Health Security Agency, at six different concentrations (1000, 500, 250, 125, 62.5, 31.25  $TCID_{50}/mL$ , where  $TCID_{50}$  stands for the median tissue culture infectious dose). We ran the same qPCR assay and determined the tentative  $LoD$  and analytical sensitivity.

### 3 | Results

#### 3.1 | In Silico Inclusivity Test for MPXV Pan-Specific Primers (B15L and F3L)

We found that both B15L and F3L primers were highly successful in amplifying MPXV across the four sub-clades (Figure 2a). Both assays achieved 100% in silico-predicted sensitivity for MPXV across all subclades, including 393 Clade Ia, 55 Clade Ib, 25 Clade IIa, and 217 Clade IIb genomes.

We found > 90% sequence similarity for all primers and probes (Figure 2b,c). Specifically, all B15L and F3L primers had 100% sequence similarity with the genomic targets, except three outliers for each. B15L probe had a consistent 96% sequence similarity with the genomic targets across all sub-clades. F3L probes had a consistent 100% sequence similarity with the genomic targets across all-subclades except the median sequence similarity for sub-Clade IIa was 96%.

#### 3.2 | In Silico Sensitivity and Specificity Test for MPXV Clade-Specific Primers (B1R)

We found that B1R primers and probes were highly specific for MPXV Clade I (Figure 2d). The median predicted amplicon length for both sub-Clade Ia was 134 bp and Ib was 134 bp, and that for sub-Clade IIa and IIb was 2379 bp and 2398 bp, respectively. All 393 Clade Ia and 55 Clade Ib were predicted to amplify, while none of the 25 Clade IIa and 217 Clade IIb genomes were predicted to amplify. Thus, the sensitivity and specificity for B1R assay was 100%.

#### 3.3 | In Silico Cross-Reactivity Test With Other Non-target Organisms

We analyzed the sequences of primers and probes for homology with full-length genomic sequences for 40 non-target high-priority organisms as above. Homology was found between primers and Poxviridae viruses, more specifically, buffalopox, camelpox, cowpox, and mousepox viruses (Figure 3a-c), where some primers were found to have homology hits in blast in all genomes. However, for the vast majority of them, the average sequence similarity was sufficiently low, except for B1R forward primer, which shared a 96% similarity with all buffalopox, cowpox virus, and mousepox viruses (Figure 3d-f).

We predicted that the only potential off-target amplification would be B15L on cowpox virus. Out of the five genomes tested, two genomes (HQ407377.1 and KY369926.1) showed > 80% sequence similarity with all forward primer, probe, and reverse primer of B15L (Supplementary Table 7).

### 3.4 | Standard Curve and Assay Performance

MPXV Clade I synthetic DNA was used to create a standard curve and evaluate the performance of the real-time PCR assay. The detection of the real-time PCR reactions was linear over six 10-fold dilutions ( $2 \times 10^6$  to  $2 \times 10^1$  copies/reaction) with a correlation coefficient 1.0, for both MPXV pan-specific primers and Clade I-specific primer (Figure 4a and Supplementary Table 8). Due to the high variance of  $C_t$  value at low copy number, the data of  $C_t$  value at 2 copies/reaction was omitted in plotting the standard curve. Amplification efficiency was high

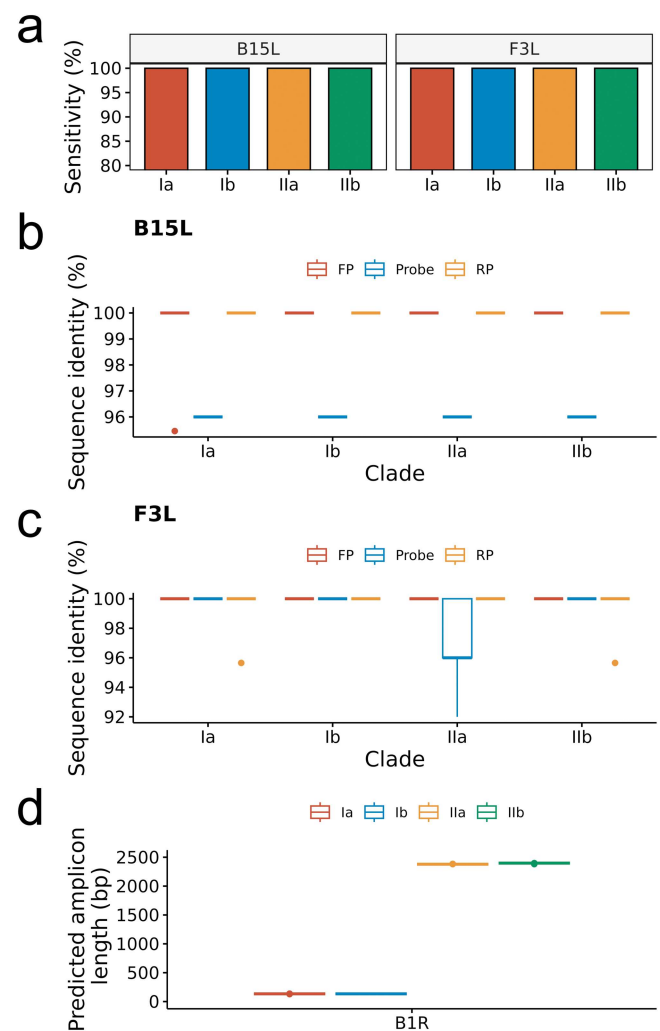


**FIGURE 2 |** (a) In silico-predicted sensitivity for B15L and F3L across four MPXV sub-clades, calculated as the number of potential amplification successes divided by the total number of genomic sequences tested; and sequence identity for forward primer (FP), probe, and reverse primer (RP) for (b) B15L and (c) F3L across four MPXV sub-clades and two genomic databases (GISAID and Nextstrain). (d) Potential amplicon length using B1R primers across four MPXV sub-clades.

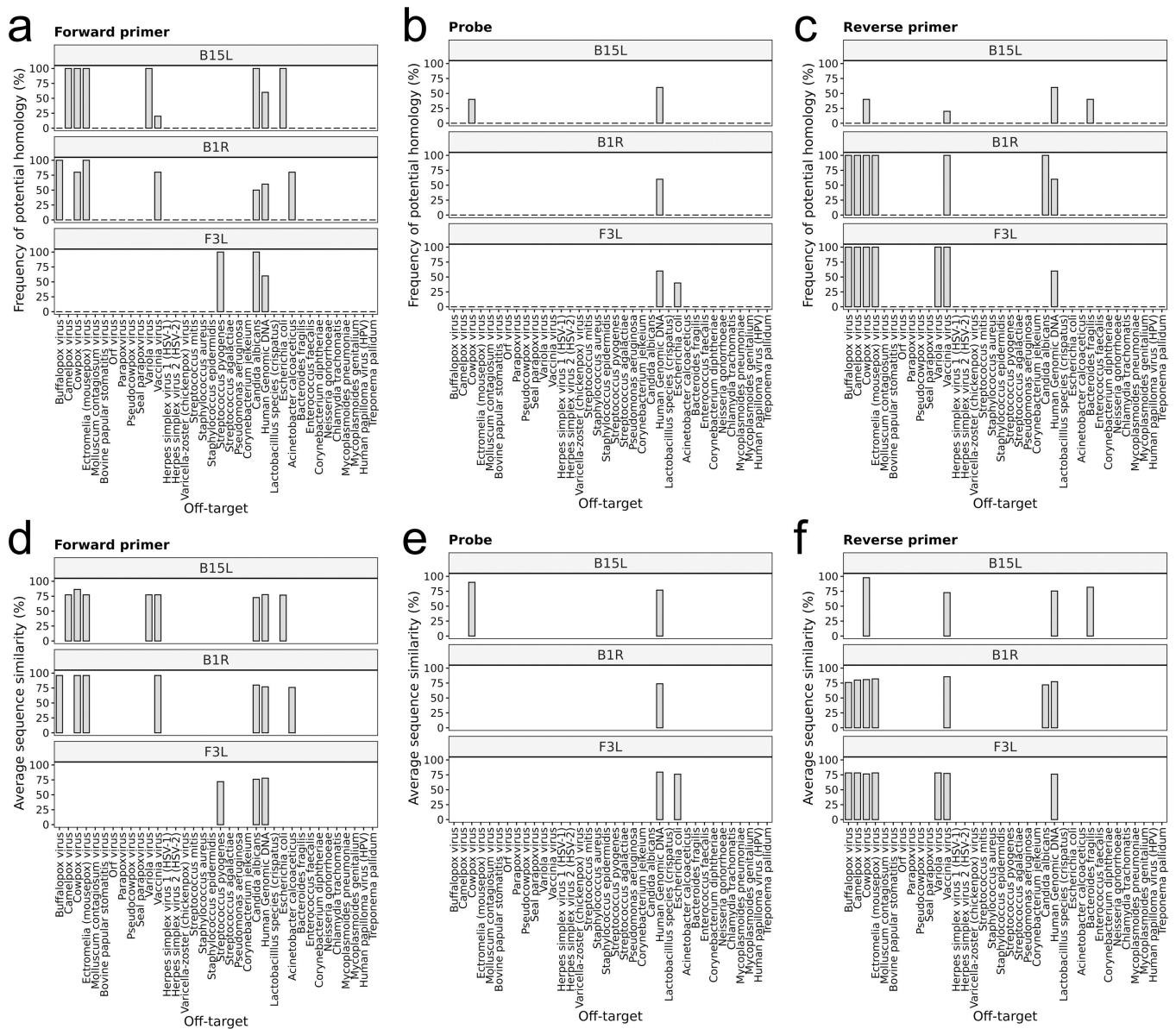


**FIGURE 3** | Frequency of homology hits between (a) forward primer, (b) probe, and (c) reverse primer for B15L, B1R, and F3L and the genomic sequences of each non-target organism ( $N = 5$ , except for organisms that did not have five representative genomes available). The list of non-target organisms was determined from the relevant WHO guideline on mpox testing. Average sequence similarity between (d) forward primer, (e) probe, and (f) reverse primer for B15L, B1R, and F3L and the genomic sequences of each non-target organism ( $N = 5$ , except for organisms that did not have five representative genomes available). The list of non-target organisms was determined from the relevant WHO guideline on mpox testing.

for both primer sets, in which all of them were 90%–110%. No false positive was observed in the triplicated reactions, indicating the reliability of the proposed real-time PCR assays.

### 3.5 | In Vitro Analytical Sensitivity for B15L, F3L, and B1R

To determine the tentative LoD of each primer set in standard laboratory settings, real-time PCR assays were triplicated with MPXV synthetic standard over six concentrations ( $2 \times 10^4$ ,  $2 \times 10^3$ ,  $2 \times 10^2$ ,  $2 \times 10^1$ ,  $2 \times 10^0$ , and  $2 \times 10^{-1}$  copies/reaction). All primer sets could successfully amplify the target at an input amount of 2 copies, the tentative LoD (Figure 4b and Supplementary Table 9). To confirm the experimental sensitivity of

each primer set, all primer sets demonstrated 100% sensitivity when repeated for 20 reactions at an input amount of 2 copies (equivalent to 100 copies/mL), confirming the analytical LoD in standard laboratory condition (Figure 4c and Supplementary Table 10).

### 3.6 | In Vitro Specificity of MPXV Clade I-Specific Assay B1R

To evaluate the specificity of MPXV Clade I-specific primer, real-time PCR was performed by using MPXV Clade II synthetic standard. Pan-specific assay (B15L + F3L) successfully detected 2000 copies of MPXV Clade II synthetic standard, while Clade I-specific primer (B1R) showed no amplification (Figure 4d).

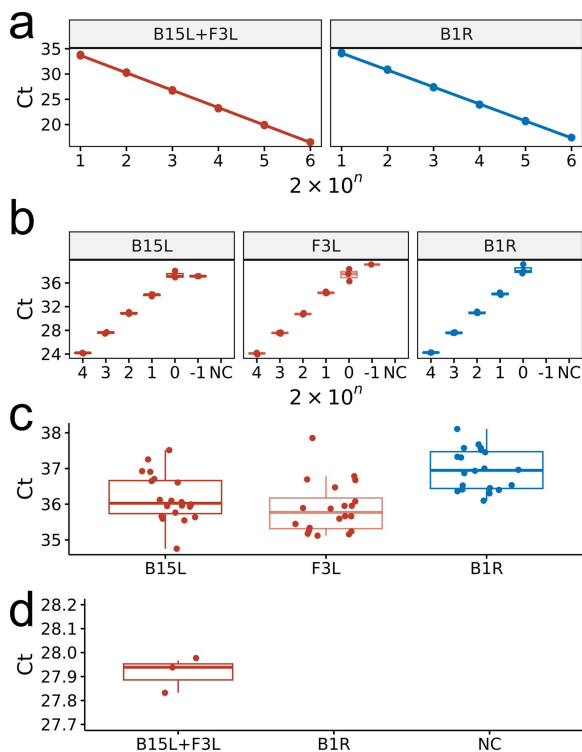


**FIGURE 4** | (a) Standard curve of real-time PCR  $C_t$  value against copy numbers of MPXV synthetic standard for pan-specific B15L + F3L primers and clade-specific B1R primers. The experiment was triplicated. (b) Tentative limit of detection (LoD) determined by real-time PCR  $C_t$  value against the copy number of MPXV synthetic standard. The experiment was triplicated. (c) Analytical sensitivity confirmed by real-time PCR of 20 replicates at the tentative LoD. (d) Analytical specificity of Clade 1-specific B1R on MPXV Clade II synthetic standard. NC denotes negative control.

The triplicated experiment confirmed the specificity of the MPXV Clade-I specific primer to be 100%.

### 3.7 | Clinical Validation of Analytical Sensitivity

For MPXV Clade I synthetic standard, we successfully detected positive signals in all triplicates at 3, 2.5, 2, 1.5, and 1 copies/reaction for B15L + F3L pan-specific assay and at 3, 2.5, and 2 copies/reaction for B1R Clade I-specific assay (Figure 5a and Supplementary Table 11). We thus estimated the tentative LoD for Clade I to be 2 copies/reaction (equivalent to 100 copies/mL). We further validated the LoD with 20 replicates. All replicates gave positive signals and thus confirmed the analytical sensitivity with high confidence (Figure 5b and Supplementary Table 12).

For MPXV Clade II synthetic standard, we successfully detected positive signals in all triplicates at 3, 2.5, 2, 1.5, and 1 copies/reaction for B15L + F3L pan-specific assay (Figure 5c and Supplementary Table 13). We thus estimated the tentative LoD for Clade II to be 1 copy/reaction (equivalent to 50 copies/mL). We further validated the LoD with 20 replicates. All replicates gave positive signals and thus confirmed the analytical LoD with high confidence (Figure 5d and Supplementary Table 14).

Probit regression models estimated even lower LoD. For MPXV Clade I, the regression-estimated  $LoD_{95}$  was 0.63 copies/

reaction for the pan-specific B15L + F3L assay and 1.88 copies/reaction for the clade-specific B1R assay. For MPXV Clade II, the regression-estimated  $LoD_{95}$  for the B15L + F3L assay was 0.63 copies/reaction. However, notably, for the pan-specific assay, detection transitioned sharply from 0% at 0 copies/reaction to 100% at  $\geq 1$  copy/reaction. Under such near-step-function behavior, regression-based LoD values are mathematically interpolated between discrete experimental concentrations and therefore reflect model-derived estimates rather than directly observed detection thresholds. It was infeasible and biologically irrelevant to have standards below 1 copy/reaction to better estimate regression-based LoD, therefore the primary LoD values reported in this study follow EP17-A2 verification.

For MPXV Clade II irradiated virus, we successfully detected positive signals in all triplicates at 1000, 500, and 250  $TCID_{50}$ /mL for B15L + F3L pan-specific assay (Figure 5e and Supplementary Table 15). We thus estimated the tentative LoD for Clade II to be 250  $TCID_{50}$ /mL. We further validated the LoD with 20 replicates. All replicates gave positive signals and thus confirmed the analytical LoD with high confidence (Figure 5f and Supplementary Table 16).

None of the replicates at any concentration of Clade II standard gave positive signals for B1R Clade I-specific assay, thus confirming the perfect specificity to differentiate MPXV clades.

## 4 | Discussion

This study presents an integrated pan-specific and clade-specific diagnostic assay suitable for near-point-of-care detection of human mpox. The assay has been validated through in silico analyses using a comprehensive genomic database, and through in vitro experiments using synthetic standards, including a test of the analytical LoD.

Our assay included two new target regions, pan-specific B15L and clade-specific B1R, and a verified pan-specific F3L. The function of B15L (IL-1 beta inhibitor) gene is not yet reported but other IL-1 beta inhibitors might interfere with host cell signaling pathways, further aiding the virus in evading immune detection and response [22]. The B1R gene encodes for a BTB-Kelch-domain protein and has a frameshift mutation and a within-gene deletion in Clade I MPXV [23], and thus initiates translation at a different start codon between Clade I and IIB MPXV, resulting in different fragments of the protein. It is also suggested a close homologue of B1R gene might inhibit the  $NF\kappa B$  pathway and stimulates CD8 + T cell proliferation but such a function in MPXV is yet to be confirmed [24]. The F3L encodes an enzyme with a double-stranded RNA binding domain and might be responsible for a broad spectrum of antiviral immune responses [25] and circumventing apoptosis to achieve productive replication [24] in the host.

Through in silico approaches, we have validated that the MPXV pan-specific assays targeting B15L and F3L showed perfect sensitivity to historical and contemporary MPXV genomes across different lineages of sub-clades. Most importantly, our clade-specific B1R assay is predicted to have high sensitivity and specificity to Clade I MPXV. Therefore, when combined with the use of either B15L and F3L as the pan-specific assay, our approach allows for clade differentiations, where Clade I would yield positive signals for both B1R and B15L/F3L, and Clade II

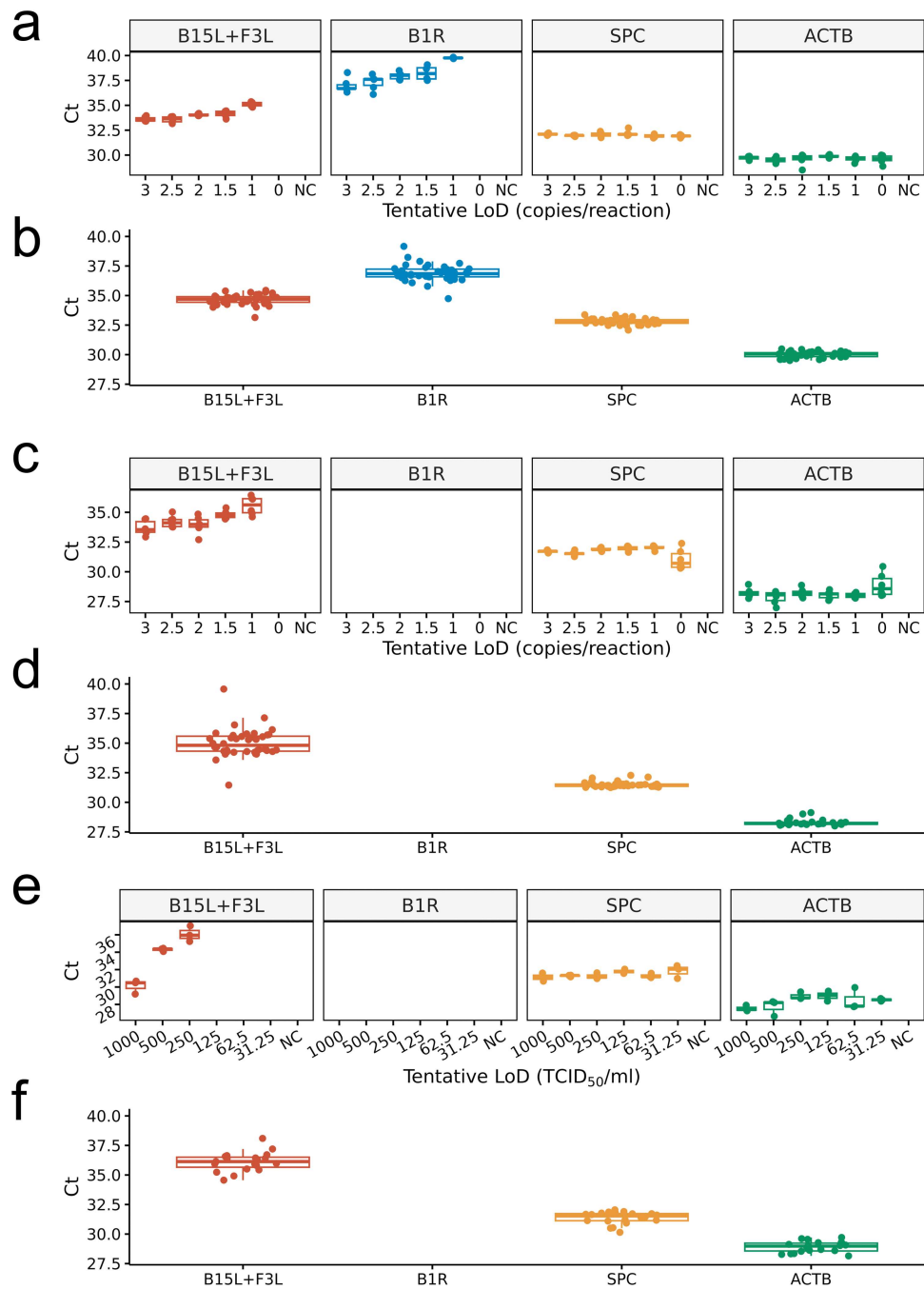


**FIGURE 5** | (a) Tentative limit of detection (LoD) for MPXV Clade I synthetic standard determined by real-time PCR  $C_t$  value against copy number of standard. The experiment was triplicated. (b) Analytical sensitivity for MPXV Clade I synthetic standard confirmed by real-time PCR of 20 replicates at the tentative LoD. (c) Tentative limit of detection (LoD) for MPXV Clade II synthetic standard determined by real-time PCR  $C_t$  value against copy number of standard. The experiment was triplicated. (d) Analytical sensitivity for MPXV Clade II synthetic standard confirmed by real-time PCR of 20 replicates at the tentative LoD. (e) Tentative limit of detection (LoD) for MPXV Clade II irradiated virus determined by real-time PCR  $C_t$  value against TCID<sub>50</sub> (median tissue culture infectious dose). The experiment was triplicated. (f) Analytical sensitivity for MPXV Clade II irradiated virus confirmed by real-time PCR of 20 replicates at the tentative LoD.

would be B1R-negative but B15L/F3L-positive. The diagnostic assay was made most efficient in a duplex real-time PCR, where each probe can be labeled with a different fluorophore (i.e., FAM and HEX). Although not tested in real-life outbreak settings, our direct real-time PCR, clade-specific assay would be directly addressing a significant gap in disease surveillance, as there is still no WHO-approved antigen-based RDT or point-of-care tests that can distinguish between mpox clades

[26]. The rapid turnaround time (<1 h) offers potential to reduce time and financial cost for clade differentiation in central laboratories.

We also thoroughly ruled out potential cross-reactivity with other closely related viruses and common contaminants in clinical samples. All B15L, F3L, and B1R showed a very high degree of specificity even among evolutionary relatives, such as buffalopox, camelpox, cowpox, and mousepox

viruses. Occasional in silico matches to B15L sequences in cowpox genomes were observed. However, cowpox is very rare and only a few hundred cases have ever been reported [27]. There is also no reported case of human-to-human transmission [28]. Therefore, a false positive result due to cowpox infection would be highly unlikely. Nonetheless, in clinical settings where orthopoxviruses may co-circulate, confirmatory testing should be considered in the case of positive results. We thus remain confident that our B15L, F3L, and B1R assays demonstrate excellent sensitivity and specificity to MPXV.

The analytical sensitivity of our assay, 2 copies per reaction for MPXV Clade I and 1 copy per reaction for MPXV Clade II, demonstrated utility in detecting extremely low amount of MPXV genomes. Our sensitivity is more superior than any assay reported on mpox, including Li et al.'s at 3.5–40.4 copies [29], Maksyutov et al.'s at 20 copies [19], Li et al.'s at 15 copies [30], Mills et al.'s at 3.3 copies [31], and Paniz-Mondolfi et al.'s at 7.2 copies [32], except Uhteg and Mostafa's also at 2 copies but theirs could not differentiate clades [33]. It should be noted, however, that these LoD values were derived under controlled experimental conditions using synthetic material, and actual performance may vary in complex clinical matrices. We also further validated the sensitivity and specificity of our assay using irradiated virus at 250 TCID<sub>50</sub>/mL. The primary LoD values reported in this study follow CLSI EP17-A2 verification criteria with  $\geq 95\%$  detection in 20 replicates, while regression-based estimates are lower but less reliable. It is therefore likely that the real analytical sensitivity of our assay may even be more superior, but we here report a more conservative value. While the ability to detect ultra-low viral loads could be advantageous in early infection or subclinical cases [31], we acknowledge that its clinical significance should be interpreted with caution, particularly in distinguishing active infection from non-infectious shedding or residual DNA.

This study establishes the analytical performance of a direct real-time PCR assay, including in silico inclusivity and specificity analyses, in vitro determination of LOD, and verification of analytical sensitivity in spiked clinical matrix. It is not a diagnostic accuracy study conducted on naturally infected clinical specimens with an independent clinical reference method. Accordingly, prevalence-dependent performance metrics such as positive predictive value, negative predictive value, and agreement statistics such as the kappa coefficient were not evaluated. Such indices require case-based sampling and comparison against a clinical reference standard, which falls beyond the analytical validation framework and objectives of the present study.

Nonetheless, we believe that the robust sensitivity and specificity of our direct, multiplex, clade-specific real-time PCR assay, which delivers results in under 1 h, is a promising diagnostic tool for use in both surveillance and outbreak settings. Our methodological approach is comparable to many other studies [31, 34–36], which offer important insight and information as the first key step to advance diagnostics in an emerging disease. Further validation using naturally infected clinical specimens and real-world implementation studies will be essential to fully establish its clinical utility and operational feasibility.

## Author Contributions

**Hong Chang:** conceptualization, investigation, validation, project administration, supervision, writing – review and editing. **Tin Hang Hung:** conceptualization, formal analysis, investigation, methodology, validation, visualization, writing – original draft. **Binbin Li:** data curation, formal analysis, investigation, writing – review and editing. **Bobby Lim-Ho Kong:** conceptualization, data curation, formal analysis, investigation, methodology, writing – review and editing. **Ashwathi Asha Madhavan:** data curation, formal analysis, investigation, writing – review and editing. **Yue Wang:** data curation, investigation, writing – review and editing. **Ming-shan Tsai:** investigation, project administration, supervision, validation, writing – review and editing. **Dan Deng:** data curation, funding acquisition, investigation, resources, writing – review and editing. **Zhanfeng Cui:** conceptualization, project administration, supervision, writing – review and editing.

## Acknowledgments

D.D. is supported by the National Natural Science Foundation of China (ref. 82173396). H.C. is supported by the OSCAR ITC for Advanced Molecular Diagnostics (ref. YZCXPT2022204).

## Ethics Statement

This study was approved by the Institutional Review Board of Shanghai Children's Medical Center (SCMCIRB-K2025018-1).

## Conflicts of Interest

T.H.H. is a scientific advisor, and H.C., B.L.H.K., and M.-S.T. are employees of ZYTCA Limited. Their conflicts of interest have been declared in the ICJME forms.

## Data Availability Statement

All sequences and data pertaining to this study can either be found in the Supplementary Information or public databases. Accession numbers have been included in Supplementary Information.

## References

1. S. Parker and R. M. Buller, "A Review of Experimental and Natural Infections of Animals With Monkeypox Virus Between 1958 and 2012," *Future Virology* 8 (2013): 129.
2. World Health Organization. 2022–24 Mpox Outbreak: Global Trends, (2024), [https://worldhealthorg.shinyapps.io/mpx\\_global/](https://worldhealthorg.shinyapps.io/mpx_global/).
3. L. Gao, Q. Shi, X. Dong, et al., "Mpox, Caused by the MPXV of the Clade IIB Lineage, Goes Global," *Tropical Medicine and Infectious Disease* 8 (2023): 76.
4. D. A. Schwartz and P. R. Pittman, "Mpox (Monkeypox) in Pregnancy: Viral Clade Differences and Their Associations With Varying Obstetrical and Fetal Outcomes," *Viruses* 15 (2023): 1649.
5. A. R. A. Saied, "Mpox Virus Clade IIB Detection in the Air," *Journal of Medical Virology* 95 (2023): e28775.
6. J. Isidro, V. Borges, M. Pinto, et al., "Phylogenomic Characterization and Signs of Microevolution in the 2022 Multi-Country Outbreak of Monkeypox Virus," *Nature Medicine* 2022 28, no. 8 28 (2022): 1569–1572.
7. W. Cho, S. Park, H. J. Kim, et al., "Clinical Characteristics and Outcomes of Patients With Mpox During the 2022 Mpox Outbreak Compared With Those Before the Outbreak: A Systematic Review and Meta-Analysis," *Reviews in Medical Virology* 34 (2024): e2508.

8. E. Dumonteil, C. Herrera, and G. Sabino-Santos, "Monkeypox Virus Evolution before 2022 Outbreak - Volume 29, Number 2—February 2023 - Emerging Infectious Diseases Journal - CDC," *Emerging Infectious Diseases* 29 (2023): 451–453.
9. E. Dumonteil, C. Herrera, and G. Sabino-Santos, "Monkeypox Virus Evolution before 2022 Outbreak," *Emerging Infectious Diseases* 29 (2023): 451–453.
10. E. H. Vakaniaki, et al., "Sustained Human Outbreak of a New MPXV Clade I Lineage in Eastern Democratic Republic of the Congo," *Nature Medicine* 30 (2024): 2791–2795.
11. World Health Organization. First Local Transmissions of Clade Ib Mpox in the WHO European Region confirmed in the United Kingdom, (2024), <https://www.who.int/europe/news/item/05-11-2024-first-local-transmissions-of-clade-ib-mpox-in-the-who-european-region-confirmed-in-the-united-kingdom>.
12. P. E. Obermeier, C. F. Plinke, A. Brinkmann, et al., "Reemergence of Clade IIB–Associated Mpox, Germany, July–December 2023," *Emerging Infectious Diseases* 30 (2024): 1416–1419.
13. K. Pritzker, "Impact of the COVID-19 Pandemic on Molecular Diagnostics," *Expert Review of Molecular Diagnostics* 21 (2021): 519–521.
14. M. Salathé, C. Althaus, N. Anderegg, et al., "Early Evidence of Effectiveness of Digital Contact Tracing for SARS-CoV-2 in Switzerland," *Swiss Medical Weekly* 150 (2020): w20457.
15. O. Puhach, B. Meyer, and I. Eckerle, "SARS-CoV-2 Viral Load and Shedding Kinetics," *Nature Reviews Microbiology* 2022 21, no. 3 21 (2022): 147–161.
16. J. Engstrom-Melnyk, P. L. Rodriguez, O. Peraud, and R. C. Hein, "Clinical Applications of Quantitative Real-Time PCR in Virology," *Methods in Microbiology* 42 (2015): 161.
17. World Health Organization. *Target Product Profiles for Tests Used for Mpox (monkeypox) Diagnosis*. (Geneva, 2023).
18. U. Samarasekera, "WHO Ramps Up Emergency Use Mpox Diagnostics," *Lancet Microbe* 6 (2025): 101051.
19. R. A. Maksyutov, E. V. Gavrilova, and S. N. Shchelkunov, "Species-Specific Differentiation of Variola, Monkeypox, and Varicella-Zoster Viruses by Multiplex Real-Time PCR Assay," *Journal of Virological Methods* 236 (2016): 215–220.
20. D. D. Djuicy, et al., "Concurrent Clade I and Clade II Monkeypox Virus Circulation, Cameroon, 1979–2022," *Emerging Infectious Diseases* 30 (2024): 432.
21. J. F. Pierson-Perry, J. E. Vaks, A. P. Durham, et al. Evaluation of Detection Capability for Clinical Laboratory Measurement Procedures; Approved Guideline—Second Edition, (2012), [www.clsi.org](http://www.clsi.org).
22. M. G. Reynolds, D. S. Carroll, and K. L. Karem, "Factors Affecting the Likelihood of Monkeypox's Emergence and Spread in the Post-Smallpox Era," *Current Opinion in Virology* 2 (2012): 335–343.
23. P. A. Desingu, T. P. Rubeni, K. Nagarajan, and N. R. Sundaresan, "Molecular Evolution of 2022 Multi-Country Outbreak-Causing Monkeypox Virus Clade IIB," *iScience* 27 (2024): 108601.
24. E. Alakunle, D. Kolawole, D. Diaz-Canova, et al., "A Comprehensive Review of Monkeypox Virus and Mpox Characteristics," *Frontiers in Cellular and Infection Microbiology* 14 (2024): 1360586.
25. Y. Wang, J. Zhang, M. Li, et al., "Transcriptome and Proteomic Analysis of Mpox Virus F3L-Expressing Cells," *Frontiers in Cellular and Infection Microbiology* 14 (2024): 1354410.
26. M. Nemer, "The World Has Responded Too Slowly to the New Mpox Outbreak - Here's What It Needs to Do Now," *Guardian* (2024), <https://www.theguardian.com/commentisfree/2024/nov/21/world-responded-slowly-mpox-outbreak>.
27. K. Świtaj, P. Kajfasz, A. Kurth, and A. Nitsche, "Cowpox After a Cat Scratch-Case Report From Poland," *Annals of Agricultural and Environmental Medicine* 22 (2015): 456–458.
28. T. F. W. Wolfs, J. A. Wagenaar, H. G. M. Niesters, and A. D. M. E. Osterhaus, "Rat-To-Human Transmission of Cowpox Infection," *Emerging Infectious Diseases* 8 (2002): 1495.
29. Y. Li, H. Zhao, K. Wilkins, C. Hughes, and I. K. Damon, "Real-Time PCR Assays for the Specific Detection of Monkeypox Virus West African and Congo Basin Strain DNA," *Journal of Virological Methods* 169 (2010): 223–227.
30. Y. Li, V. A. Olson, T. Laue, M. T. Laker, and I. K. Damon, "Detection of Monkeypox Virus With Real-Time PCR Assays," *Journal of Clinical Virology* 36 (2006): 194–203.
31. M. G. Mills, K. B. Juergens, J. P. Gov, et al., "Evaluation and Clinical Validation of Monkeypox (Mpox) Virus Real-Time PCR Assays," *Journal of Clinical Virology* 159 (2023): 105373.
32. A. Paniz-Mondolfi, S. Guerra, M. Munoz, et al., "Evaluation and Validation of an RT-PCR Assay for Specific Detection of Monkeypox Virus (MPXV)," *Journal of Medical Virology* 95 (2023): e28247.
33. K. Uhteg and H. H. Mostafa, "Validation and Implementation of an Orthopoxvirus Qualitative Real-Time PCR for the Diagnosis of Monkeypox in the Clinical Laboratory," *Journal of Clinical Virology* 158 (2023): 105327.
34. H. H. Mostafa, G. Wall, S.-C. Su, et al., "Multi-Center Evaluation of the Research Use Only NeuMoDx Monkeypox Virus (MPXV) Fully Automated Real-Time PCR Assay," *Journal of Clinical Microbiology* 62 (2024): e0002824.
35. M. N. Anahar, B. M. Shaw, D. Slater, et al., "Development of a Qualitative Real-Time RT-PCR Assay for the Detection of SARS-CoV-2: a Guide and Case Study in Setting Up an Emergency-Use, Laboratory-Developed Molecular Microbiological Assay," *Journal of Clinical Pathology* 74 (2021): 496–503.
36. B. Fung, A. Gopez, V. Servellita, et al., "Direct Comparison of SARS-CoV-2 Analytical Limits of Detection Across Seven Molecular Assays," *Journal of Clinical Microbiology* 58 (2020): e01535-20.

### Supporting Information

Additional supporting information can be found online in the Supporting Information section.

**Supplementary Figure 1:** Detection probability against number of copies per reaction for MPXV Clade I (B15L+F3L and B1R assays) and MPXV Clade II (B15L+F3L assay). Curves represent fitted probit regression models. The horizontal dashed line indicates 95% detection probability. Vertical dotted lines indicate regression-estimated LoD95.

**Supplementary Table 1:** List of 40 non-target high priority organisms from the WHO instructions and requirements for emergency use listing submission on in vitro diagnostic testing of MPXV nucleic acid (PQDx\_457 version).

**Supplementary Table 2:** Sequences and statistics for all primers and probes listed in this study.

**Supplementary Table 3:** List of 56 MPXV genomes used for multiple genome alignment and clade-specific primer design.

**Supplementary Table 4:** List of randomly selected representative genomes for each organism listed in Supplementary Table 1 for cross-reactivity analysis.

**Supplementary Table 5:** Sequences of (a) Clade I and (b) Clade II MPXV synthetic standards. Red, blue, and green sequences denote the F3L, B15L, and B1R amplicons.

**Supplementary Table 6:** List of human skin lesion samples used for the MPXV clinical negative sample matrix.

**Supplementary Table 7:** Statistics of potential off-target amplification from two cowpox virus genomes.

**Supplementary Table 8:** Ct values from real-time PCR for determination of standard curve for MPXV synthetic standards.

**Supplementary Table 9:** Ct values from real-time PCR for tentative limit of detection of MPXV synthetic standard. NC denotes negative control.

**Supplementary Table 10:** Ct values from real-time PCR for analytical limit of detection using 2 copies of MPXV

synthetic standard per reaction. NC denotes negative control. **Supplementary Table 11:** Ct values from real-time PCR for tentative limit of detection of MPXV Clade I synthetic standard spiked in clinical negative matrix. NC denotes negative control. **Supplementary Table 12:** Ct values from real-time PCR for analytical limit of detection of MPXV Clade I synthetic standard spiked in clinical negative matrix. NC denotes negative control. **Supplementary Table 13:** Ct values from real-time PCR for tentative limit of detection of MPXV Clade II synthetic standard spiked in clinical negative matrix. NC denotes negative control. **Supplementary Table 14:** Ct values from real-time PCR for tentative limit of detection of MPXV Clade II synthetic standard spiked in clinical negative matrix. NC denotes negative control. **Supplementary Table 15:** Ct values from real-time PCR for tentative limit of detection of MPXV Clade II irradiated virus spiked in clinical negative matrix. NC denotes negative control. **Supplementary Table 16:** Ct values from real-time PCR for tentative limit of detection of MPXV Clade II irradiated virus spiked in clinical negative matrix. NC denotes negative control.